CHAPTER IV

RESULTS AND DISCUSSION

In this chapter, there are three sections namely, the determination of kinetic parameters, the influence of COS concentration and temperatureon the kinetics as well as the proposed reaction mechanism.

The Selexsorb® COS used in this study was activated alumina impregnated with one or more alkali metal compounds, one or more alkaline earth metal compounds, or a mixture. There are also secret proprietary active components. They were referred to as the active metal compounds.

This investigation concentrated on the removal of COS from propylene by adsorption on Selexsorb® COS. The kinetics of COS adsorption used in this study followed case 2.1 of the Langmuir-Hinshelwood model.

$$COS \longrightarrow product \tag{4.1}$$

The rate equation for heterogeneous system is given by:

$$-r = k\,KP_A / (1 + KP_A) \tag{4.2}$$

It was assumed that the pressure of COS, (P_A) and the function $kK / (1 + KP_A)$ were represented by COS concentration (C) and rate constant (k), respectively. The elementary kinetics of general reaction was, therefore, applied for this work. The rate equation is shown as below.

$$-r = -(d\,[\,C\,]^n)\,/\,dt = k[C]^n \tag{4.3}$$

The apparent initial rate of reaction for continuous flow tube reactor is given by :-

$$-r_{COS} = (dX_{COS})/(W/F_{o,COS})$$ (4.4)

The apparent rate constant followed the Arrhenius Equation :-

$$k = k_o\, e^{(-E_a/RT)}$$ (4.5)

4.1 Determination of the Order of Reaction and Rate Constant

Experiments A to E of COS adsorption on Selexsorb® COS was performed at 313 K using 1 gram of adsorbent. The reactant flow rate was between 50 and 450 mL. min^{-1} of gaseous COS in propylene. The COS concentration varied between 1 and 5 wt. ppm. The experimental results are summarized in appendix C.

The COS conversion at the steady-state was averaged from values obtained after 20-30 minutes of reaction at each condition. The analysis results of COS concentration and the actual COS reactant flow rate for each experiment are shown in Table 4.1. The COS conversions by varying the COS concentration and space time are shown in Table 4.2.

Table 4.1   COS concentrations and the flow rate of COS as a reactant for the experiment A to E.

Experiment	COS concentration		Flow rate of COS with respect to	
	(wt. ppm)	(mol/m^3)	Propylene (mL. min^{-1})	COS (mol. s^{-1})
A	1.08	0.0338	51 to 210	2.87×10^{-07} to 1.18×10^{-06}
B	1.53	0.0479	50 to 508	3.99×10^{-07} to 4.05×10^{-06}
C	3.81	0.1190	104 to 450	2.06×10^{-06} to 8.93×10^{-06}
D	4.94	0.1550	50 to 340	1.29×10^{-06} to 8.76×10^{-06}
E	6.68	0.2090	73 to 450	2.54×10^{-06} to 1.57×10^{-05}

Table 4.2 COS conversion by varying both COS concentration and flow rate of reactant for experiment A to E.

Experiment	Absorbent wt. (gm.)	$W/F_{o,cos}$	COS Concentration. (ppb)		COS Conversion (X_{cos})
			Reactant	Product	
A1	1.0032	848	1.08	0.57	0.468
A2	0.9925	973	1.08	0.56	0.480
A3	0.9975	1230	1.08	0.54	0.500
A4	1.0176	1660	1.08	0.52	0.520
A5	1.0032	3490	1.08	0.45	0.580
B1	1.0180	251	1.53	0.78	0.492
B2	1.0017	306	1.53	0.71	0.534
B3	1.0059	413	1.53	0.60	0.610
B4	0.9919	1130	1.53	0.41	0.732
B5	1.0102	2530	1.53	0.18	0.881
C1	1.0115	113	3.81	2.35	0.381
C2	1.0142	127	3.81	2.10	0.448
C3	0.9370	154	3.81	1.77	0.535
C4	1.0077	246	3.81	1.09	0.713
C5	1.0105	489	3.81	0.75	0.804
D1	0.9951	114	4.94	2.57	0.479
D2	0.9991	129	4.94	1.96	0.604
D3	1.0438	162	4.94	1.62	0.671
D4	1.0400	269	4.94	0.54	0.891
D5	1.0118	786	4.94	0.44	0.911
E1	0.9987	64	6.68	4.10	0.387
E2	1.0119	73	6.68	3.65	0.454
E3	0.9955	114	6.68	2.40	0.641
E4	1.0119	194	6.68	1.66	0.752
E5	0.9955	391	6.68	1.16	0.827

The rate of reaction was differentially determined using plot of conversion, X_{COS} vs. space time. (Figure 4.1 to 4.5) in conjunction with equation 4.3. The initial slope (at $t = 0$) of the curve was used as the initial rate of reaction (see appendix E). The results obtained are presented in Table 4.3.

Table 4.3   Rate of reaction for the determination of order of reaction and rate constant.

Experiment	COS (mol/m^3)	r_{COS} (mol.kg-1.s-1)	ln [COS]	ln (r_{COS})
A	0.0338	9.00E-04	-3.387	-7.013
B	0.0479	2.30E-03	-3.039	-6.075
C	0.1190	4.20E-03	-2.129	-5.473
D	0.1550	4.90E-03	-1.864	-5.319
E	0.2090	8.10E-03	-1.565	-4.816
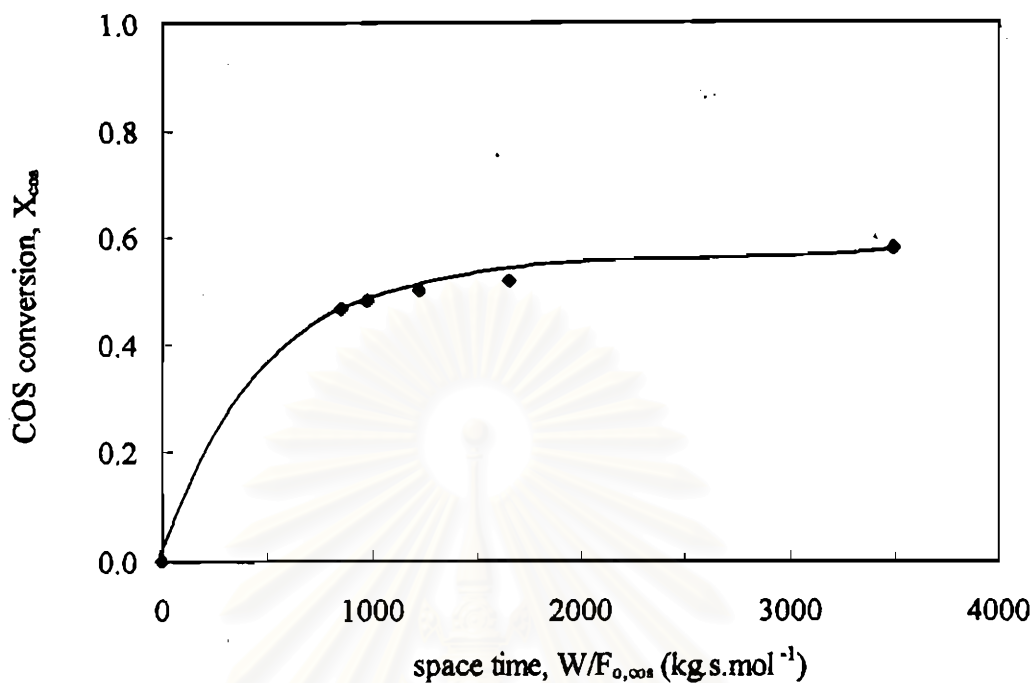
Figure 4.1 Relationship between space time and COS conversion for the adsorption at 313 K and 1.08 wt. ppm of COS reactant (experiment A).
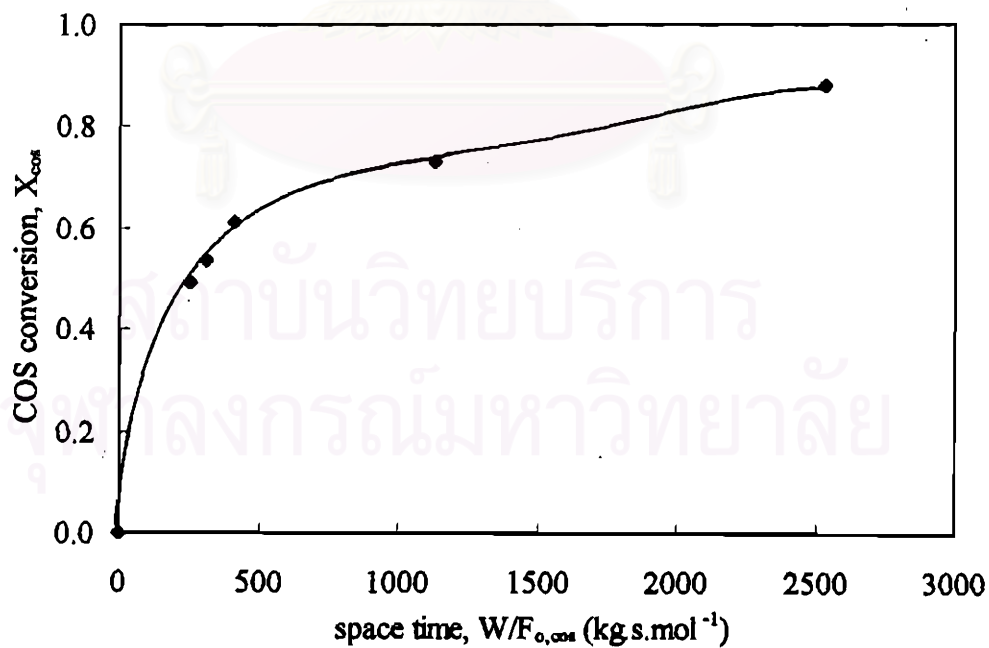
Figure 4.2 Relationship between space time and COS conversion for the adsorption at 313 K and 1.53 wt. ppm of COS reactant (experiment B).
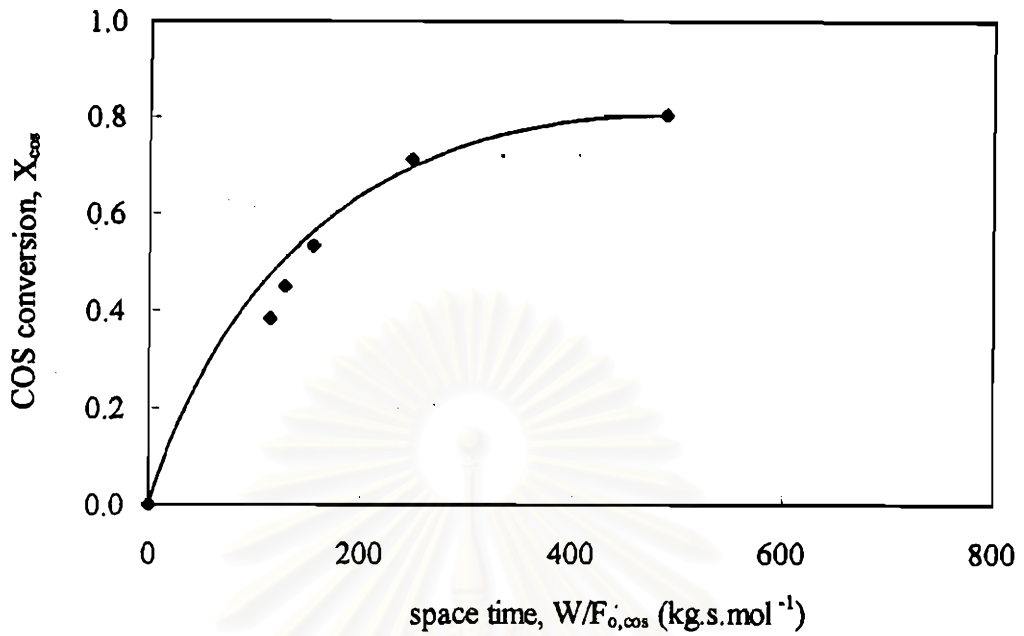
Figure 4.3 Relationship between space time and COS conversion for the adsorption at 313 K and 3.81 wt. ppm of COS reactant (experiment C).
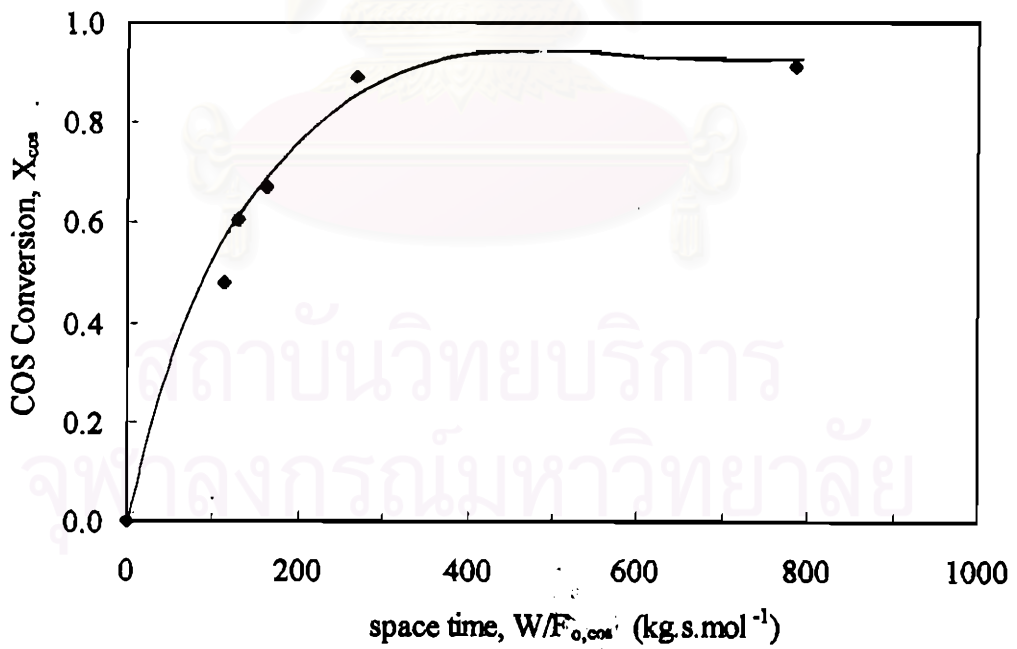

Figure 4.4 Relationship between space time and COS conversion of the adsorption at 313 K and 4.94 wt. ppm of COS reactant (experiment D).
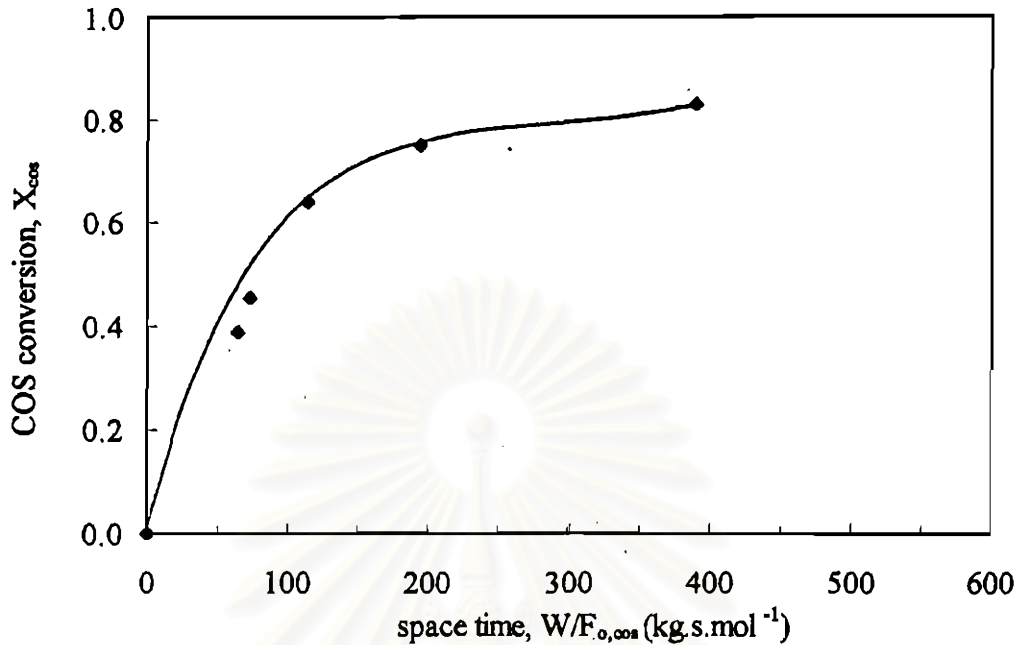
Figure 4.5 Relationship between space time and COS conversion for the adsorption at 313 K and 6.68 wt. ppm of COS reactant (experiment E).

Taking natural logarithm of equation.

$$\ln (r_{COS}) = \ln k + \ln [COS]$$

(4.6)

The $\ln(r_{COS})$ values were plotted against $\ln(COS)$ values $\ln(COS)$ in order to determine the $\ln k$ and n value (Figure 4.6) with the aid of linear regression. The values obtained are given below :

$$y \quad = \quad 1.04x - 3.24$$
$$n \quad = \quad 1.04$$
$$\ln k = \quad -3.24$$

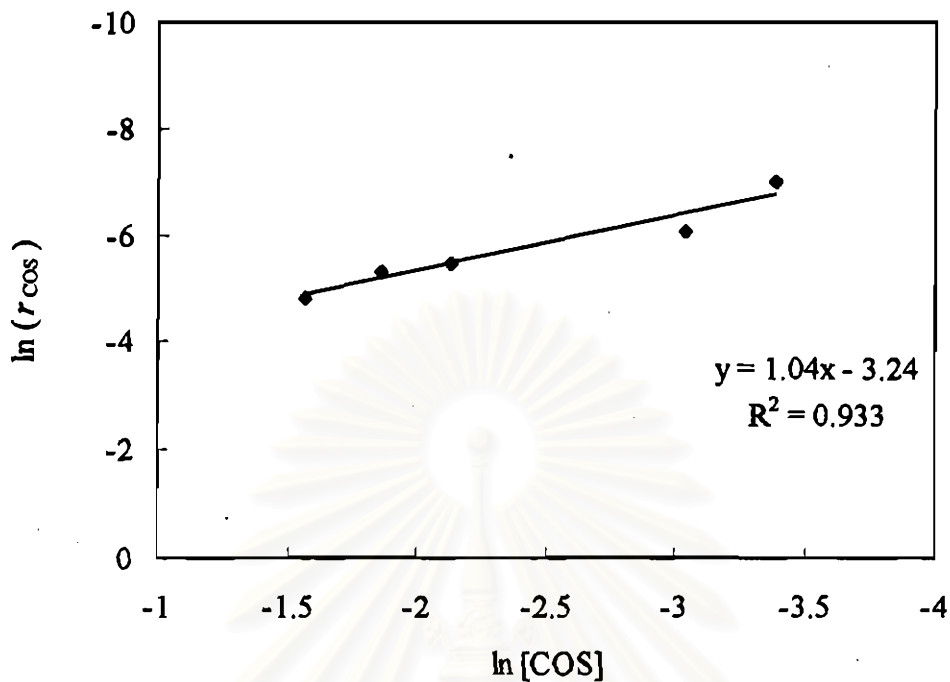**Figure 4.6** Relationship between ln [COS] and ln (r_{COS}) in order to determine the order of reaction with respect to COS.

The rate constant at 313 K obtained from the intercept of the linear equation equals to 3.92×10^{-2} $kg^{-1}.s^{-1}$ (figure 4.6)

Hence, the rate equation of COS adsorption on Selexsorb COS is related to the order of COS concentration as follow :

$$-r_{COS} = k \, [COS]^{1.04} \qquad (4.7)$$

The COS adsorption on Selexsorb® COS (alumina impregnated with metal compounds) is the first order of reaction in COS concentration. The COS concentration range used for this study is 1 to 7 wt. ppm. It was described that , for the reaction rate that was the first order at sufficiently low value of reactant pressure , the system followed the Langmuir-Hinshelwood model in the case of unimolecular (case 2.1) as below expression [5].

$$- r = kKP_A / 1 + KP_A \qquad (4.8)$$

In this study, The adsorption was operated in the low COS concentration which could be represented to COS pressure. It is clear that the order of reaction of COS adsorption on Selexsorb® COS follows the Langmuir-Hinshelwood model.

The COS adsorption with primary and secondary amine in aqueous solution was a study for COS removal of which the order of reaction was similar to this study. It was concluded that the overall reaction rate was first order in COS concentration [2].

4.2 Determination of Activation Energy

In order to determine the activation energy of the COS adsorption, the adsorption reaction was carried out at 303, 313, 318, 323, and 333 K at constant concentration. The experimental results have been summarized in appendix C. The analysis results of COS reactant concentration and the actual COS reactant flow rate for each experiment are shown in Table 4.4. The COS conversions by varying temperature and space time are shown in Table 4.5.

Table 4.4 Temperatures and flow rate of COS at 1.02 wt. ppm of COS feed concentration.

Experiment	Temperature (K)	Flow rate of COS with respect to	
		Propylene (mL. min^{-1})	COS (mol. s^{-1})
F	303	50 to 402	2.65×10^{-07} to 2.13×10^{-06}
G	313	60 to 450	3.18×10^{-07} to 2.38×10^{-06}
H	318	50 to 450	2.65×10^{-07} to 2.38×10^{-06}
I	323	50 to 457	2.65×10^{-07} to 2.42×10^{-06}
J	333	50 to 452	2.65×10^{-07} to 2.39×10^{-06}

Table 4.5   Effect of adsorbent weight : feed rate ratio on the COS conversion.

| Experiment	Absorbent weight (gm.)	$W/F_{o,cos}$	COS Concentration. (ppb)		COS conversion (X_{cos})
			Reactant	Product	
F1	1.0155	471	1.02	0.52	0.489
F2	1.0124	619	1.02	0.48	0.523
F3	0.9952	743	1.02	0.41	0.591
F4	1.0128	1230	1.02	0.38	0.630
F5	1.0197	3740	1.02	0.24	0.762
G1	0.9952	449	1.02	0.32	0.681
G2	1.0186	540	1.02	0.27	0.732
G3	0.9959	757	1.02	0.22	0.783
G4	0.9981	1260	1.02	0.12	0.881
G5	0.9922	3130	1.02	0.04	0.957
H1	1.0123	425	1.02	0.25	0.749
H2	0.9913	533	1.02	0.17	0.830
H3	1.0110	750	1.02	0.13	0.872
H4	1.0198	1270	1.02	0.08	0.919
H5	0.9954	3810	1.02	0.04	0.957
I1	0.9952	414	1.02	0.23	0.770
I2	1.0119	557	1.02	0.22	0.783
I3	1.0156	764	1.02	0.18	0.821
I4	0.9946	1240	1.02	0.16	0.838
I5	1.0122	3750	1.02	0.12	0.881
J1	1.0194	418	1.02	0.13	0.868
J2	0.9936	547	1.02	0.10	0.906
J3	0.9959	769	1.02	0.08	0.923
J4	1.0173	1270	1.02	0.09	0.965
J5	1.0106	3750	1.02	0.04	0.962
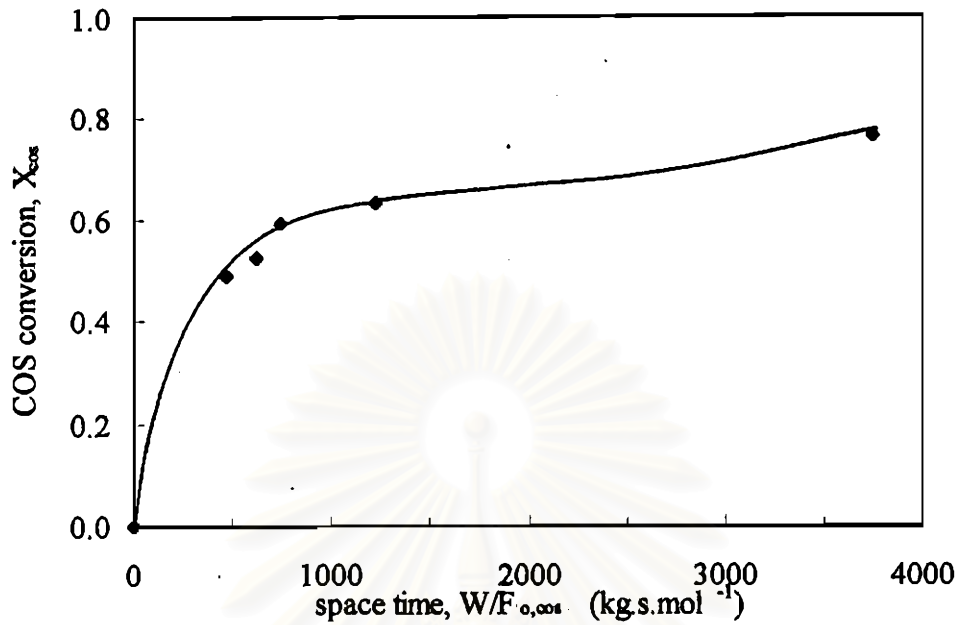
Figure 4.7   Relationship between space time and COS conversion to determine r_{COS} for the adsorption at 303 K and 1.02 wt. ppm of COS reactant (experiment F).
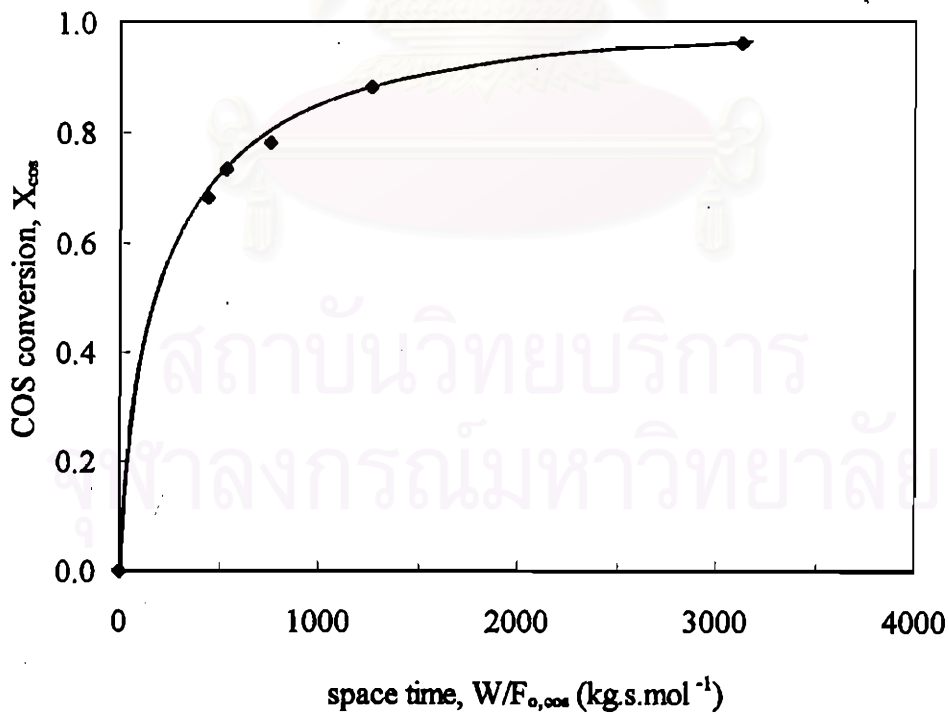

Figure 4.8   Relationship between space time and COS conversion to determine r_{COS} for the adsorption at 313 K and 1.02 wt. ppm of COS reactant (experiment G).
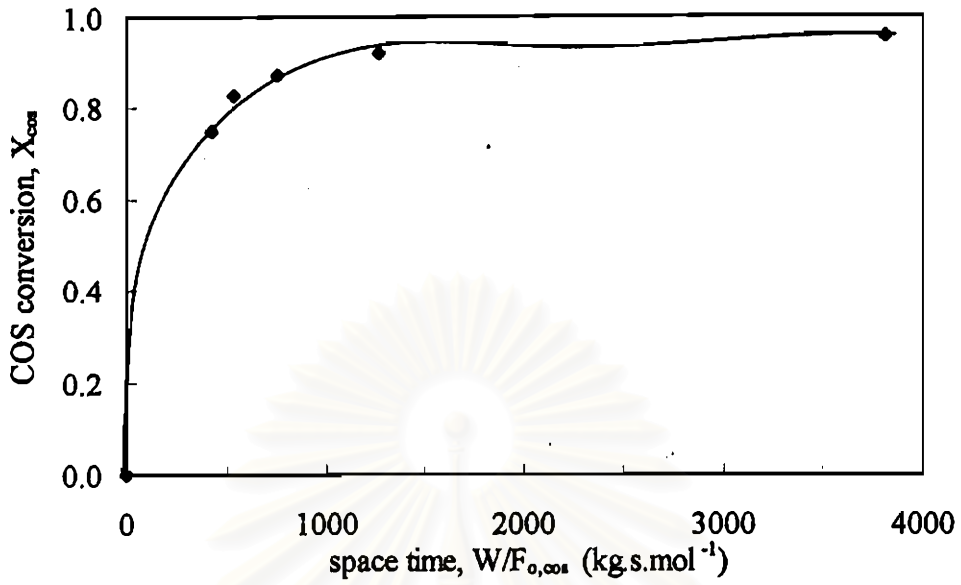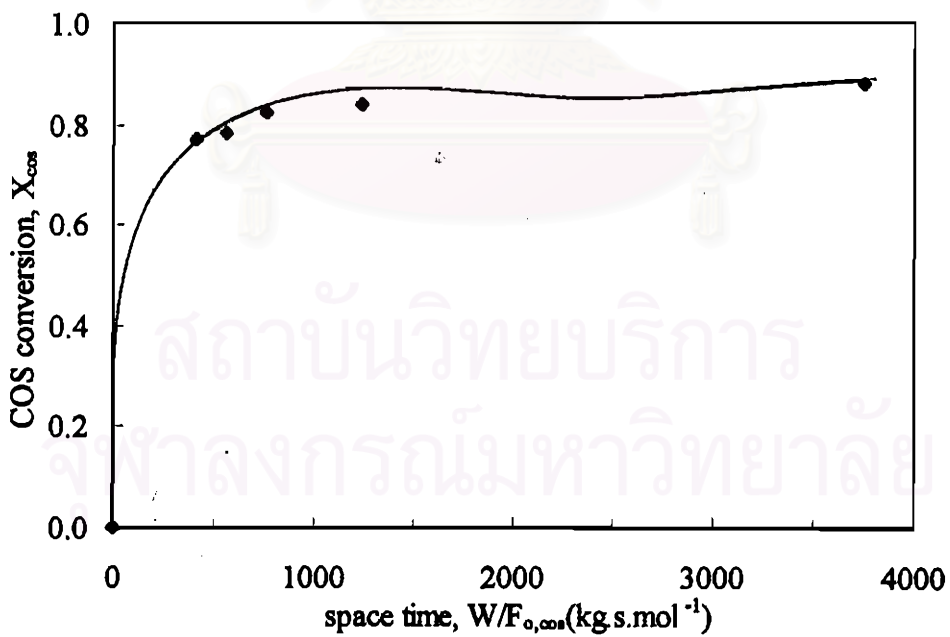
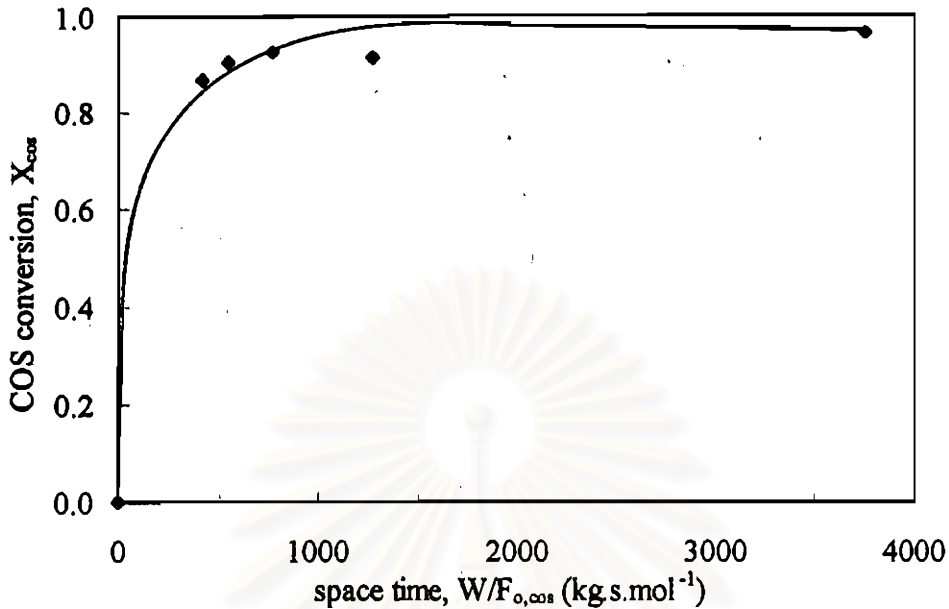**Figure 4.9**   Relationship between space time and COS conversion to determine r_{COS} for the adsorption at 318 K and 1.02 wt. ppm of COS reactant (experiment H).

Figure 4.10   Relationship between space time and COS conversion in to determine r_{COS} for the adsorption at 323 K and 1.02 wt. ppm of COS reactant (experiment I).

Figure 4.11 Relationship between space time and COS conversion in to determine r_{COS} for the adsorption at 323 K and 1.02 wt. ppm of COS reactant (experiment J).

Table 4.6 Experimental rate of reaction and rate constant (k) obtained at different reaction temperature.

Experiment	Temp. (K)	$-r_{COS}$ (mol.kg^{-1}.s^{-1})	k (sec^{-1})	1/T	ln k
F	303	0.0016	0.0576	3.30×10^{-03}	-2.8540
G	313	0.0026	0.0935	3.19×10^{-03}	-2.3693
H	318	0.0030	0.1080	3.14×10^{-03}	-2.2262
I	323	0.0032	0.1150	3.10×10^{-03}	-2.1616
J	333	0.0036	0.1300	3.00×10^{-03}	-2.0439

Note : The rate constant at various temperatures were calculated using the following expression :

$$- r_{COS} = k[COS]^{1.04} \tag{4.8}$$

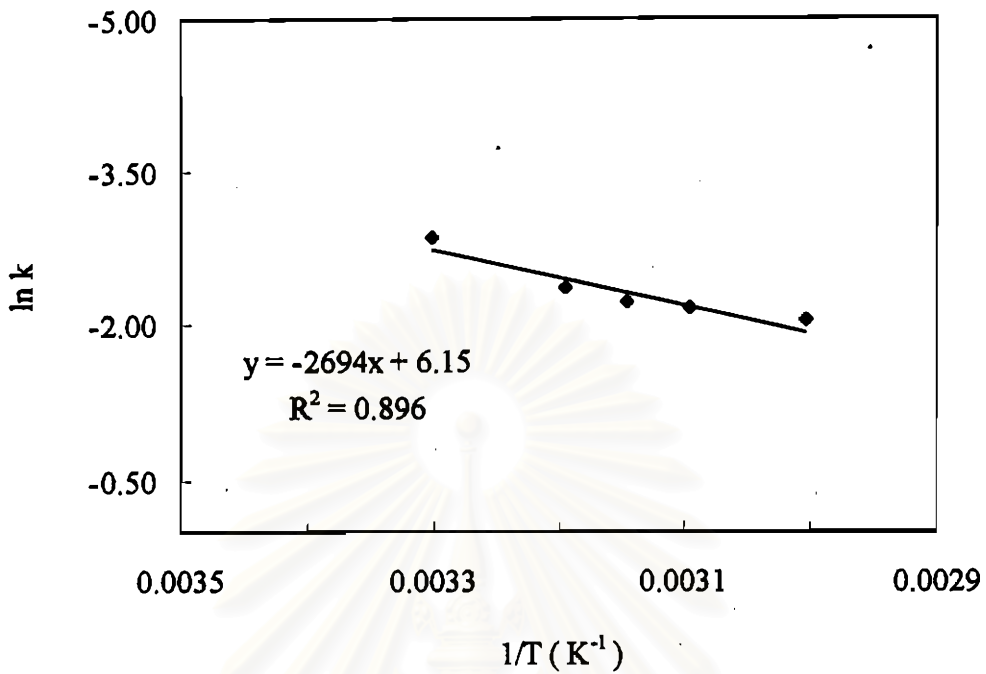**Figure 4.12**   Arrhenius plot for the COS adsorption on Selexsorb® COS in order to determine E_a and k_0

From the Arrhenius equation

$$k \quad = \quad k_0\, e^{(-E_a/RT)} \tag{4.9}$$

and

$$\ln k \quad = \quad \ln k_0 - (E_a/R)/(1/T) \tag{4.10}$$

The slope and intercept of this Arrhenius plot (Figure 4.12) are $(-E_a/R)$ and $\ln k_0$, respectively. The resulting apparent activation energy, E_a and frequency factor, k_0 are 22.4 kJ.mol^{-1} and 468.7 kg$^-$1.sec^{-1}, respectively. The rate law of COS adsorption on Selexsorb® COS now becomes :-

$$r_{COS} \quad = \quad 468.7 e^{-22.4/RT}\,[COS]^{1.04} \tag{4.10}$$

4.3   Limitations to External Transfer

The first step of heterogeneous catalysis mechanism, the external mass transfer of carbonyl sulfide to the surface of Selexsorb®COS was considered from this experiment.   The detecting of limitation to external transfer was considered the variation of COS conversion with the changes in the COS concentration   at the constant COS flow rate..

From the plot of the COS conversion versus COS concentration of each ratio of absorbent weight to mass flow rate of reactant shown in Figure 4.13, the COS conversion varied significantly with the changes in the COS concentration changes at constant COS flow rate, it was considered that the apparent rate was limited by the external transfers.

Generally there is no external diffusion control for a high surface area of adsorbent (more than 200 $m^2.g^{-1}$). Nevertheless in the case of low COS concentration in propylene gas, its mass diffusivity is very low ($\mathcal{D}_{eff}$ of argon-oxygen mixture = 0.188 , $\mathcal{D}_{eff}$ of COS in propylene = 0.0702). The COS reactant gradually diffused from bulk phase into the adsorbent surface. The external diffusion is a slow step,. hence, it becomes one of rate limiting step of this reaction mechanism.
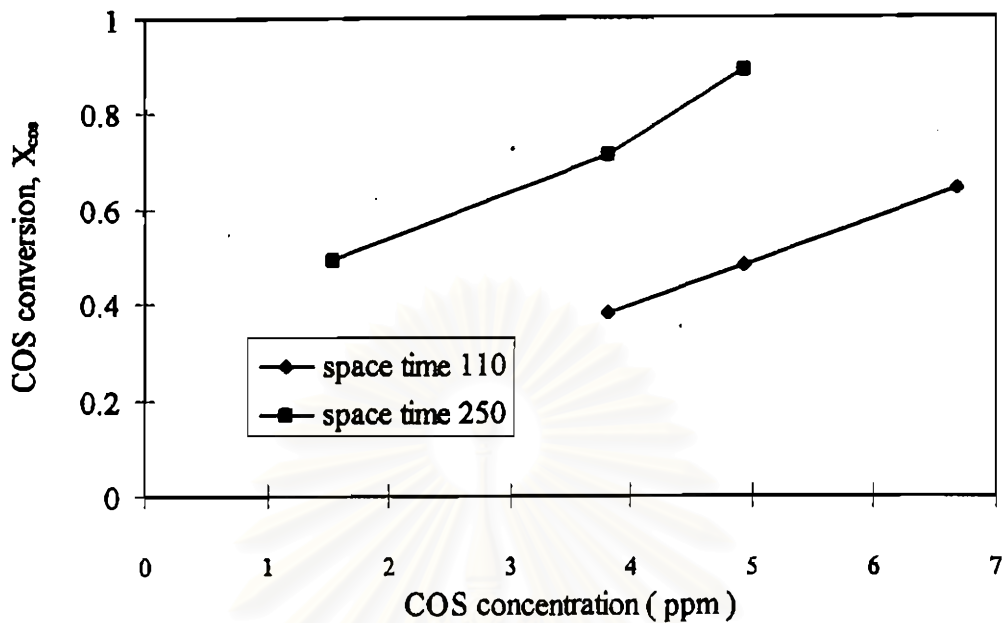
Figure 4.13 Test of external diffusion limitation to reaction .

4.4   Limitations to Internal Transfer.

The first mechanism of heterogeneous catalysis is external mass transfer from bulk phase of COS reactant, the diffusion into pore is the next step called internal transfer. As a result of no experimental results from varying the particle size of the adsorbent, it was not considered the detecting of limitation to internal tranfer using Thiele module, ϕ as equation   (4.11)

$$\Phi = \eta\phi^2 = (d_p^2 \rho_g v) (4 \, . \mathcal{D}e.C_b) \tag{4.11}$$

Nevertheless, the Weisz-Prater criterion was used for the detection of the internal mass transfer limitations.

if $\dfrac{(rate) \, (V_p/S_{p,ext})^2}{\mathcal{D}e.Cg}$ > 1 then there is the internal diffusion limitation

if $<< 1$ then there is a chemical reaction control.

Minimum as maximum rate of reaction from this study are 9×10^{-4} mol.s^{-1} and 8.1×10^{-3} mol.s^{-1}, respectively.

$$V_p \text{ of Selexsorb}^{@} \text{ COS} \quad = \quad 0.5 \text{ cm}^3/\text{g}$$

$$S_{p,ext} \text{ of Selexsorb}^{@} \text{ COS} \quad = \quad 270 \text{ m}^2/\text{g}$$

$$\mathfrak{D}_{eff} \quad = \quad 7.03 \times 10^{-2} @ 313 \text{ K}$$

$$C_g \quad = \quad \text{concentration gradient}$$

Table 4.7 Test of internal diffusion limitation to the COS conversion.

Apparent Rate (mol.s^{-1})	Concentration (mol/m^3)	The value from Weisz-Prater Criterion	Interpretation
9.0×10^{-4}	0.0338	1.30×10^{-6}	No internal diffusion limitation
8.1×10^{-3}	0.2090	1.89×10^{-6}	No internal diffusion limitation

Based on the result of Weisz-Prater criterion that is less than 1, the adsorption of carbonyl sulfide on Selexsorb® COS is not limited by internal diffusion. On the other hand the mechanism controlled this reaction should be the chemical reaction.

Unfortunately, the active metal compounds impregnated onto the activated alumina of Selexsorb® COS is still not disclosed. It is difficult to propose the exact chemical reaction, but possible chemical reaction may be the production of a metal sulfide as below :

$$\text{COS + active metal compounds} \longrightarrow \text{metal-sulfide} \qquad (4.12)$$
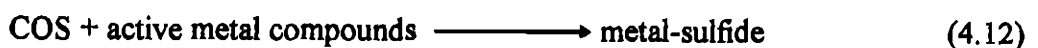
There are two reasons to support this proposed chemical reaction. Firstly, Selexsorb® COS used can be regenerated at a temperature of 250 °C and pressurized up to 20 barg with nitrogen [3] in order to break the metal-sulfide bond. Secondly, it was found that there was one product of this reaction, hydrogen sulfide, that was found in all effluent flow. This implied that the chemical reaction is an important mechanism.

4.5   Influence of Space Time on COS Conversion

The COS conversion was expected to increase with increasing space time. On the other hand, lower COS reactant mass flow increases the contact time of COS reactant to the adsorbent surface. There will be insufficient contact time to complete the reaction as if the mass flow was higher.

It was noticed that at higher space time($W/F_{0,cos} > 500$ kg.s.mol^{-1}) there was no influence of space time. The COS conversion remained constant even the space time changes. Whereas the COS conversion were changed dramatically at a lower space time ($W/F_{0,cos} = 50$-500 kg.s.mol^{-1}) (Figure 4.14). It was shown that the contact time between COS reactant and the active metal compounds was prolonged at a higher space time, $W/F_{0,cos}$ or the lower COS flow rate, $F_{0,cos}$ .Therefore the kinetics of COS adsorption should be studied at the lower space time ($W/F_{0,cos} = 50$-500 kg.s.mol^{-1}) in order to observed the COS conversion obviously.
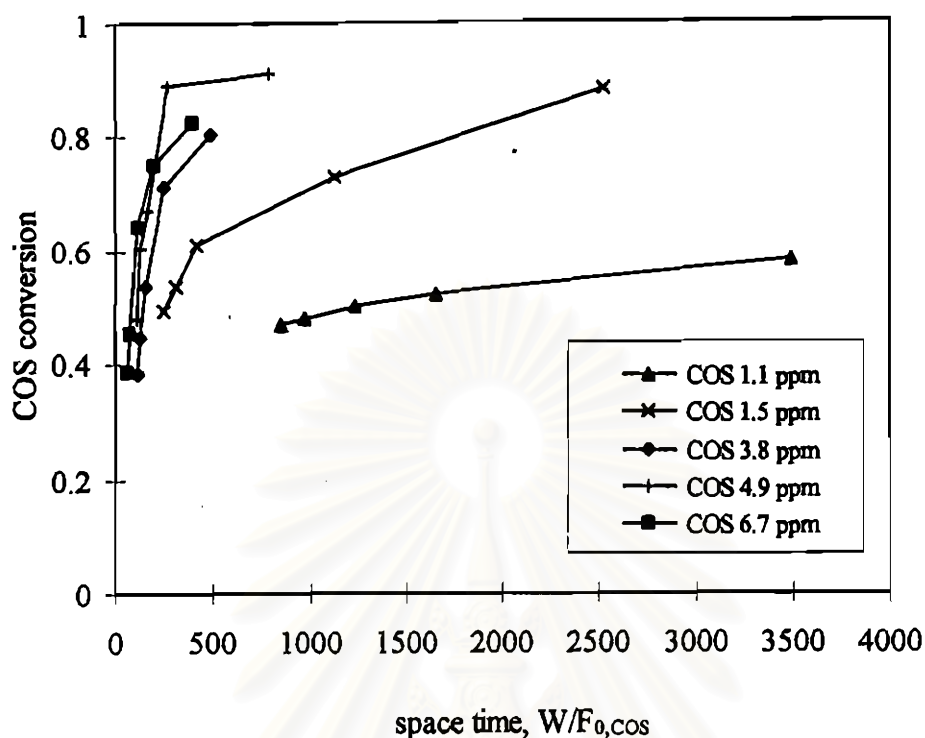
Figure 4.14 Influence of space time ($W/F_{0,cos}$) on COS conversion

4.6 Influence of COS Concentration on Reaction Rate

The influence of COS reactant concentration on the COS adsorption was studied so that the reaction rate control could be clarified. Two cases were considerd (1) when the space time was increased, and (2) when the space time was kept constant at 110 and 250 kg.s.mol^{-1} For the first case, the effect of COS concentration on reaction rate was enhanced as shown in Figure 4.15. In the second case, the COS conversion increased with the COS concentration increase as shown in Figure 4.16.

As typical reaction, the increase of reactant concentration is going to disturb the chemical equilibrium, the rate of reaction could be faster. It is induced that the COS concentration is a parameter for increasing the rate of reaction.
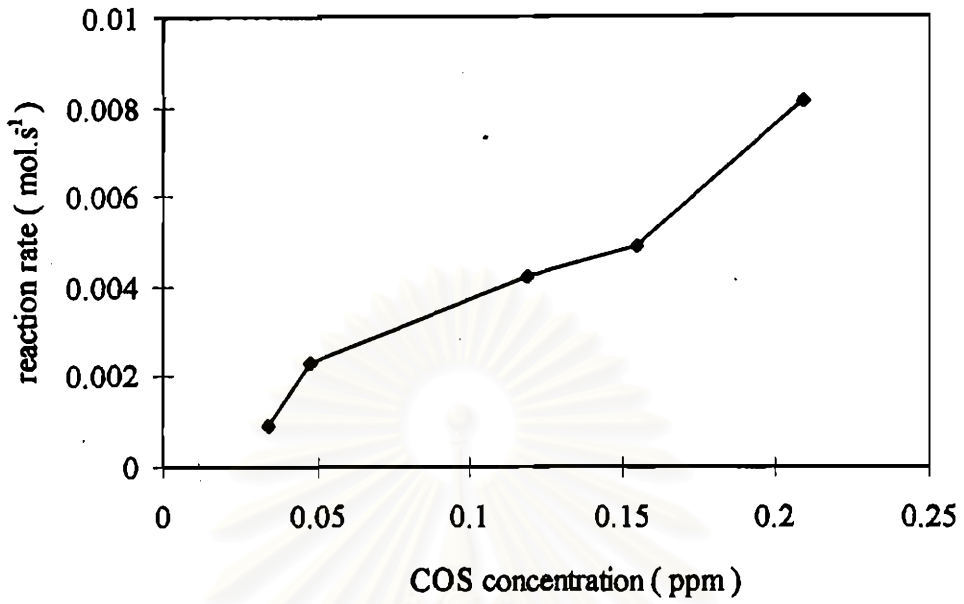
Figure 4.15 Influence of COS concentration on the rate of reaction at different space times
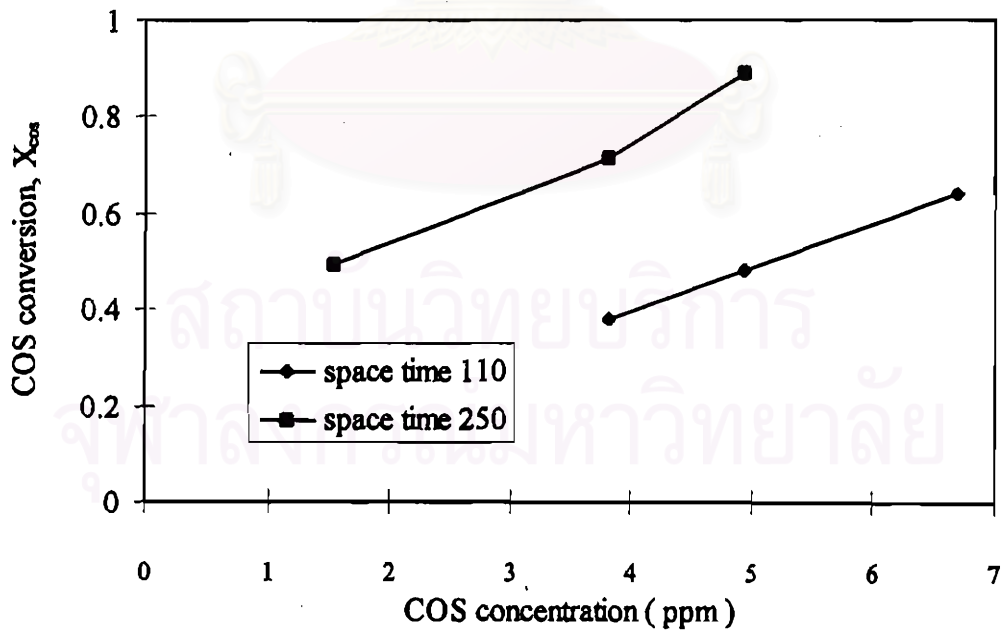

Figure 4.16 Influence of COS concentration on the COS conversion at the constant space time

4.7 Influence of Temperature on Reaction Rate

The influence of reaction temperature on the COS adsorption was considered in order to study the trend of the optimum reaction temperature. The reaction rate increased with an increase in the temperature as different space time (Figure 4.17), Furthermore, the COS conversion also showed an increasing trend with increasing temperature at constant space time shown in Figure 4.18. The results showed that the temperature increases resulted in an increase in the rate constant higher which in term increased the COS conversion and reaction rate higher also.
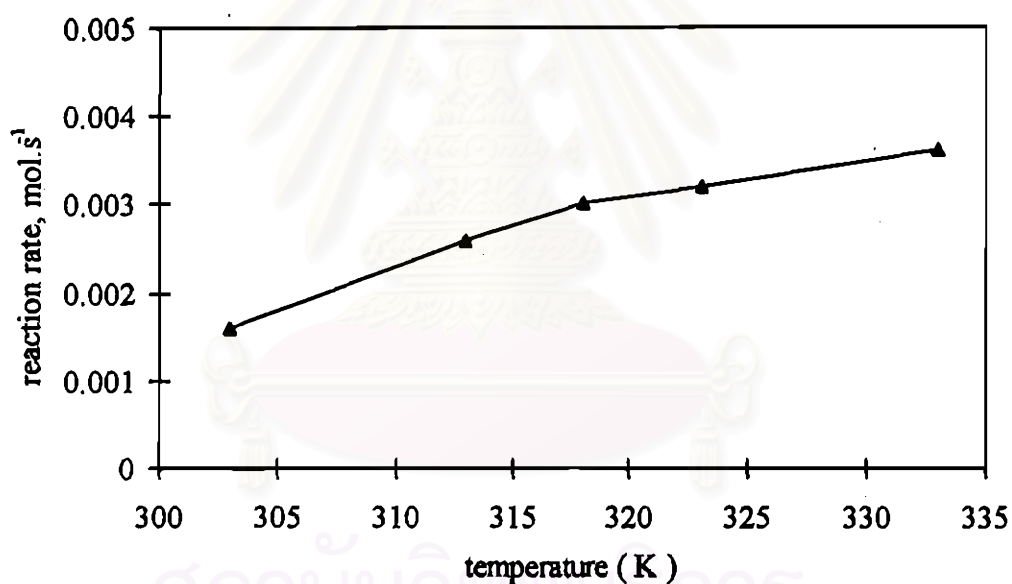

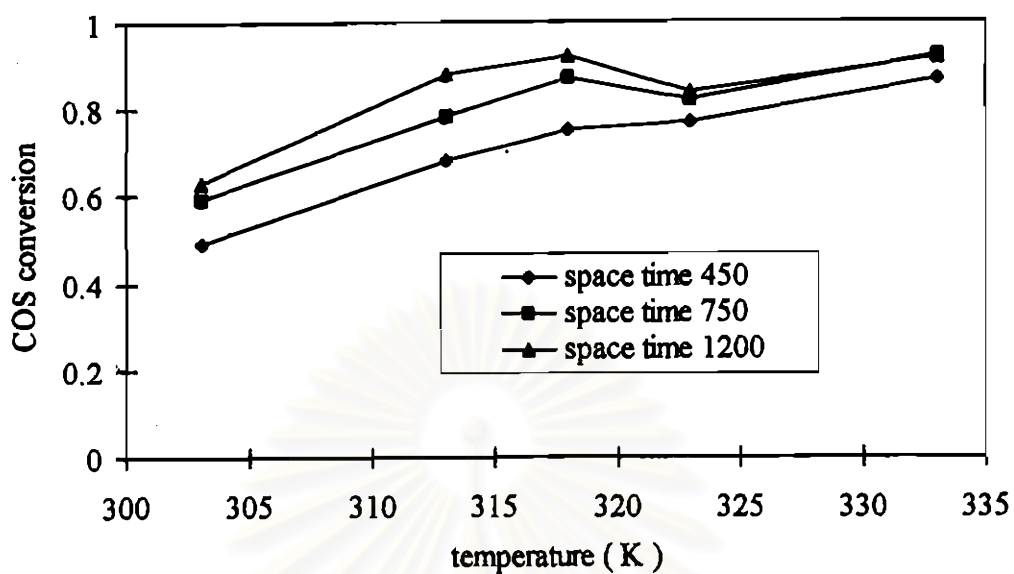**Figure 4.17** Influence of the temperature on the reaction rate at the different space time

Figure 4.18 Influence of the temperature of the COS conversion at the constant space time.